14th International Symposium on Turbulence and Shear Flow Phenomena (TSFP14)
Heidelberg, Germany, July 28–31, 2026

INFLUENCE OF COHERENT STRUCTURES ON TKE DECAY

Ankit Gautam & Tim Berk
Department of Mechanical and Aerospace Engineering
Utah State University
4130 Old Main Hill, Logan, Utah, 84322, USA
tim.berk@usu.edu

ABSTRACT

The decay rate of turbulent kinetic energy (TKE) in nominally homogeneous turbulence exhibits substantial variability across experiments and simulations, with reported power-law exponents spanning $m \approx 1.0$–2.0. In this study, we investigate the role of coherent structures in this variability using a synthetic-jet-driven turbulence facility in which coherent vortical motions are systematically introduced through asymmetric forcing. Increasing coherent content reduces the apparent decay exponent from $m \approx 1.4$ to $m \approx 0.66$.

To isolate the underlying mechanism, a Proper Orthogonal Decomposition (POD)-based framework is developed to identify and remove coherent modes based on their temporal decay behavior and cross-realization correlation. After removing these modes, the remaining stochastic component exhibits consistent decay exponents in the range $m = 1.2$–1.45, largely independent of forcing conditions.

These results demonstrate that a small number of energetic coherent structures can significantly bias measured TKE decay rates, providing a mechanistic explanation for the variability of decay exponents reported in the literature.

INTRODUCTION

The decay of turbulent kinetic energy (TKE) has been the subject of debate over the last century. In homogeneous isentropic turbulence (HIT), when assuming preserved self-similarity during the decay, a power-law scaling can be derived—and is commonly accepted—of the form

$$k(t) \sim (t - t_0)^{-m}, \tag{1}$$

where $k = u_1'^2 + u_2'^2 + u_3'^2$ is twice the turbulent kinetic energy, m is the power-law exponent and t_0 is a temporal virtual origin. A wide range of theoretical and empirical values for m exist. Kolmogorov derived $m = 10/7 \approx 1.4$ (Kolmogorov, 1941) while the Birkhoff-Saffman model predicts $m = 6/5 = 1.2$ (Saffman, 1967). John *et al.* (2022) recently summarized empirical decay exponents from 38 studies, showing that experimental wind tunnel data ranges between $m = 1.0$–1.5 while simulations range from 1.0–2.0. To our knowledge, four studies have experimentally investigated TKE decay in zero-mean-flow conditions, yielding decay rates of 1.2–1.9 (Hwang & Eaton, 2004; Goepfert *et al.*, 2010; Esteban *et al.*, 2019; Gorce & Falcon, 2023).

The spread in the obtained values of m precludes the validation of a universal decay rate. Several possible reasons have been proposed, including time-history effects of production mechanisms, confinement effects—which get worse as the integral scales grow during decay, Reynolds number effects, inhomogeneity, and anisotropy (see, e.g. Esteban *et al.* 2019; John *et al.* 2022).

In the present work, we focus on a different mechanism: the existence of coherent structures in the flow. Conventional Reynolds decomposition separates the velocity field into a time-averaged and a fluctuating component—the latter implicitly assumed to be stochastic. The problem is that this does not distinguish between stochastic fluctuations and coherent structures. Both contribute to the velocity variance, and thus to TKE, but their decay behaviors differ significantly. Coherent vortices decay slowly, while stochastic turbulence dissipates more rapidly through the cascade. If coherent components are not separated, the apparent decay exponent m can be biased, potentially contributing to the spread in reported values.

The objective of this study is therefore twofold: (i) to demonstrate experimentally how coherent structures influence TKE decay in a jet-driven turbulence box, and (ii) to develop a decomposition-based methodology for isolating the true stochastic decay rate. We use proper orthogonal decomposition (POD) to identify coherent modes in the flow, which we use as a proxy for coherent structures. Using a selective POD-filtering procedure we isolate the decay of the stochastic turbulence. To test the robustness of our method, we inject coherent structures through asymmetric inhomogeneous forcing. As expected, these structures reduce the overall decay rate of turbulent kinetic energy. We then show that—while the overall decay rate is reduced—the stochastic components still decay with expected exponents which fall in-between theoretical estimates by Birkhoff-Saffman and Kolmogorov.

METHODS

Facility and Flow Diagnostics

The experiments were conducted in a 0.6 m cubic turbulence box shown in figure 1. The front, back, and top of the box consist of transparent acrylic to enable optical measurements. Two opposite faces are populated with 32 synthetic-jet actuators each, arranged in a grid of 6×6 (with the corners absent). Each actuator consists of a small cavity with a 1-cm circular orifice on the box-side and a Visaton KT100V4 loudspeaker on the outside. These subwoofer speakers were selected for their high-performance at low actuation frequency. Speakers are operated at a nominal power of 24 W while their frequency is dynamically randomized between 11.25–45 Hz using a "sunbathing" algorithm (Bellani & Variano, 2014). This operation sends randomized fluidic pulses which break down into turbulence inside the box. Forcing was applied for 60 seconds prior

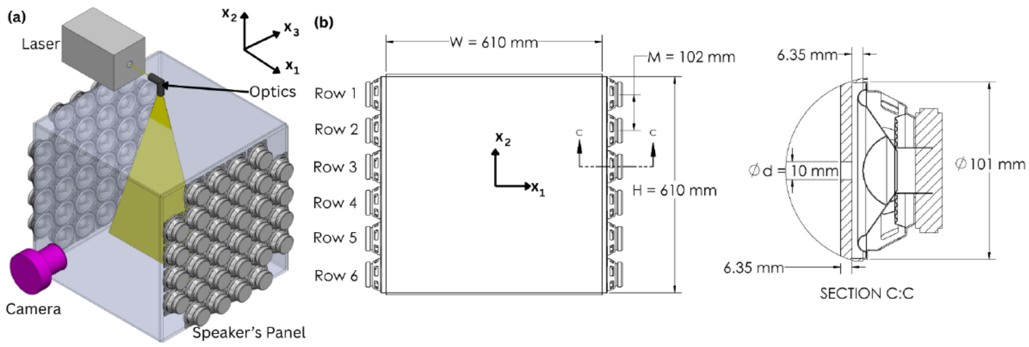

Figure 1: (a) Overview of experimental setup; (b) cross-sectional view as observed by the camera and sectional view of synthetic jet actuator.

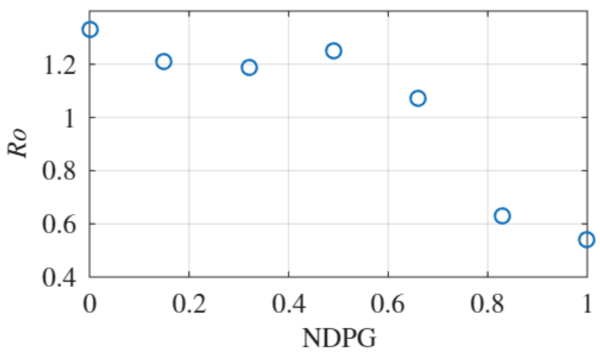

Figure 2: Rossby number Ro as function of the non-dimensional power gradient NDPG. $Ro > 1$ indicates turbulence-dominated while $Ro \ll 1$ indicates significant coherent vortical structures.

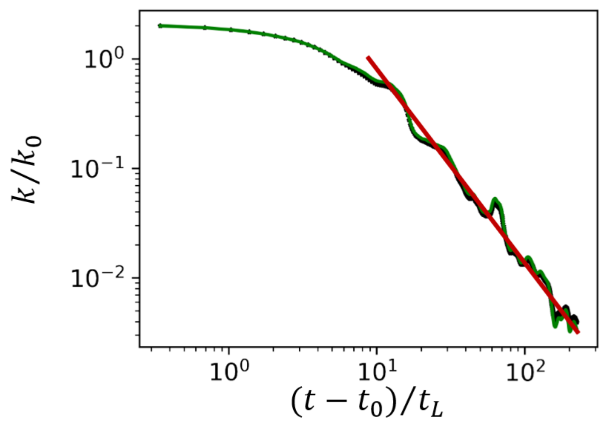

Figure 3: Representative decay of turbulent kinetic energy k as function of time t in dissipating turbulence. t_0 is the virtual origin, $k_0 = k(t_0)$, and t_L is the eddy turnover time.

to each measurement, ensuring a statistically stationary state. Then, 24 seconds of this steady state were measured, followed by 24 seconds of decay.

Velocity fields in the central plane were measured using planar particle image velocimetry (PIV). Prior to experimental runs, the turbulence box was seeded using a LaVision Aerosol Generator (producing sub-micron DEHS droplets). Seeding was illuminated using a dual-cavity Nd:YLF laser. Images were captured at 50 Hz using a LaVision CX-5 (5 MP) camera, yielding a field of view of 10 cm by 12 cm at the center of the box. Vector fields were computed with a multi-pass interrogation algorithm with a final pass of 32×32 pixels, resulting in 1.6 mm spatial resolution. Each dataset contained 2400 fields, spanning both forced and decaying phases.

Parameter Space

At nominal power, homogeneous nearly-isotropic turbulence is generated with $Re_\lambda = 182$. Isotropy ratio ($u_{\mathrm{rms}}/v_{\mathrm{rms}} = 1.27$), mean flow factor ($\overline{u}/u_{\mathrm{rms}} = 0.07$), and homogeneity deviation ($2\sigma/u_{\mathrm{rms}} = 0.09$) are all similar to other two-panel facilities (Carter *et al.*, 2016; Nezami *et al.*, 2023).

To probe the role of coherent vortices, the two facing jet panels were operated asymmetrically with one panel at nominal power while a power gradient was applied to the second panel. This gradient is quantified using a non-dimensional power gradient $\mathrm{NDPG} = \left(P_{\mathrm{top}} - P_{\mathrm{bottom}}\right)/P_{\mathrm{top}}$. This metric ranges from $\mathrm{NDPG} = 0$ (no power gradient, i.e. all speakers at nominal power) to $\mathrm{NDPG} = 1$ (power gradient from nominal power at the top to zero power at the bottom).

The presence of coherent structures is quantified using a modified Rossby number, which takes the ratio of turbulent fluctuations over vorticity fluctuations, $Ro = u_{rms}/(\omega_{rms} L)$, where L is the integral lengthscale. With increasing presence of coherent structures, the Rossby number decreases. As shown in figure 2, the Rossby number is above unity (i.e. turbulence-dominated) for $\mathrm{NDPG} < 0.7$ but sharply drops for larger NDPG, indicating the dominance of coherent vortical structures in the latter cases.

RESULTS

A typical decay curve for the turbulent kinetic energy k is shown in figure 3. Initially, turbulence decays slowly before transitioning into a power-law decay (indicated by the red line). A key difficulty in fitting the decay law lies in the selection of the virtual origin t_0 and the fitting start time t_{start}. We follow established approaches in the literature (Lavoie *et al.*, 2007; Hearst & Lavoie, 2014; Esteban *et al.*, 2019).

The virtual origin t_0 is determined by minimizing the variability of the fitted decay exponent m over a range of fitting intervals. Specifically, we perform least-squares regression over varying t_{start} and t_0, and select the value of t_0 that yields the smallest standard deviation in m. This procedure yields a consistent value across all cases, and we adopt $t_0 = 0.40$ s.

The fitting start time is chosen as the earliest time for which the fitted exponent remains approximately constant

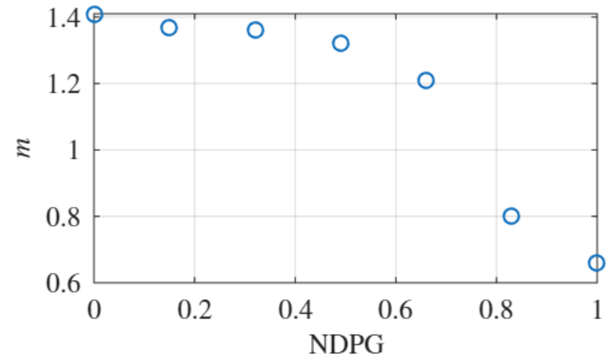

Figure 4: Fitted decay coefficient m as function of non-dimensional power gradient NDPG for the seven cases.

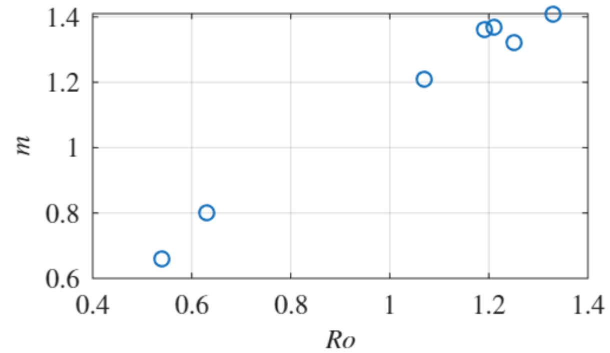

Figure 5: Fitted decay coefficient m as function of Rossby number Ro for the seven cases.

(within $\pm 0.5\%$), while also satisfying $t_{start} \geq 10\, t_L$ to ensure self-similar decay.

Decay coefficients obtained using this fitting procedure are shown in figure 4. In absence of an applied power gradient (NDPG $= 0$) the decay coefficient is $m \approx 1.4$, in-line with theoretical predictions as well as prior empirical results. For small power gradients ($0 <$ NDPG < 0.5) the decay coefficient shows a slight monotonic decrease. For larger power gradients—especially for NDPG > 0.7—the decay coefficient decreases sharply to $m \approx 0.66$.

This decay coefficient correlates strongly with the Rossby number, shown in figure 5. For $Ro > 1$—indicative of turbulence-dominated flow—the decay coefficient is $m = 1.2$–1.4, equivalent to theoretical and empirical values. In contrast, for smaller Rossby numbers—indicative of flow dominated by coherent vortical motions—the decay coefficient is sharply reduced. Overall, a relatively linear and monotonic trend exists between m and Ro.

This trend suggests an influence of coherent vortical motions on the decay of turbulent kinetic energy. We *hypothesize* a superposition of coherent structures on top of the stochastic turbulent motions. In order to separate the decay dynamics of the two, we utilize proper orthogonal decomposition (POD) which mathematically separates the flow into modes and ranks them based on their kinetic energy. While these are mathematically recurring modes, we use them as proxies for coherent structures or stochastic components.

POD is applied to the steady-state turbulence (i.e. before the decay phase). The obtained modes are then projected onto the decay phase, resulting in decay coefficients $m^{[j]}$ for each of the steady-state modes ($[j]$). These modal decay coefficients are shown as function of normalized modal energy in figure 6.

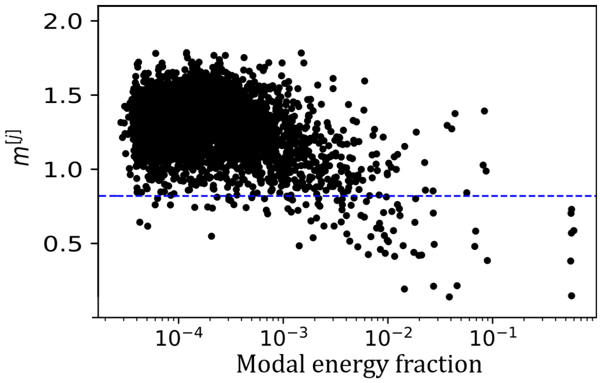

Figure 6: Modal decay coefficients $m^{[j]}$ as function of normalized modal energy for each steady-state POD mode for the $Ro = 0.54$ case. Dashed blue line indicates $m = 0.81$, the lowest reported empirical decay coefficient (John *et al.*, 2022).

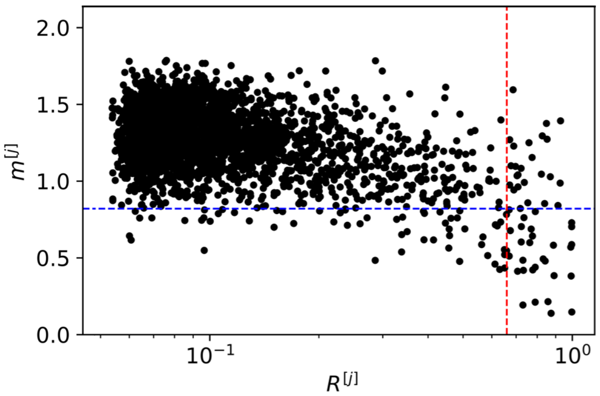

Figure 7: Modal decay coefficients $m^{[j]}$ as function of modal correlation $R^{[j]}$ for the $Ro = 0.54$ case. Dashed blue and red lines indicate $m = 0.81$ and $R = 0.66$, respectively.

A large number of low-energy modes have decay coefficients of $m^{[j]} = 0.9$–1.7. In contrast, the distribution for the $O(10^2)$ highest-energy modes is skewed downward. The modal decay coefficient of the highest energy modes is below $m^{[j]} < 0.8$—lower than decay rates of stochastic turbulence as reported in the literature (John *et al.*, 2022).

Figure 6 shows that certain modes decay faster than others. However, the wide distribution for low-energy (presumed stochastic) modes suggests that decay rate alone cannot be used to distinguish between modes reflecting stochastic turbulence and coherent structures, respectively. Instead, we use an additional metric: the modal correlation $R^{[j]}$ (Butcher & Spencer, 2019). For each power gradient (e.g. each Ro) the experiment is repeated a total of six times—resulting in six separate sets of POD modes. For each of these sets, the POD modal shapes are correlated with the shapes of the other five sets, leading to correlation values $R^{[j]}$ for each POD mode. High correlation values indicate "coherent" modes which occur multiple times in independent datasets.

The modal decay rate $m^{[j]}$ is shown as function of modal correlation $R^{[j]}$ in figure 7. We identify coherent, slow-decaying modes using the thresholds $m^{[j]} < 0.81$ and $R^{[j]} > 0.66$. In an effort to apply these thresholds conservatively, we label only those modes that satisfy both thresholds (i.e. the bottom right quadrant) as "coherent" and all other modes as "stochastic". We then partially reconstruct velocity fields using these separate sets of POD modes, resulting in velocity fields assumed to consist of coherent structures and stochastic turbulence, respectively.

We determine the turbulent-kinetic-energy decay rates of these partially reconstructed velocity fields using the procedure outlined above, leading to separate sets of decay rates m. The decay rates of the full velocity fields, the reconstructed "coherent" velocity fields and reconstructed "stochastic" velocity fields are shown for each of the seven power-gradient cases in figure 8. We note that the partial reconstruction changes the Rossby number of the remaining flow, shifting each case along the horizontal axis.

The partial reconstruction using only the modes identified as "coherent" (orange squares) has lowered the Rossby number for each case, indicating that modal coherence is related to vortical content. A significant and non-obvious result is that the trend of Ro versus m already observed in the original velocity fields (blue circles) is maintained in these partially reconstructed fields.

In contrast, the velocity fields reconstructed with the "stochastic" modes (yellow triangles) have shifted the Rossby number upward, indicative of dominant turbulent fluctuations compared to coherent vortical motions. Rather than extending the observed Ro–m relationship (i.e. leading to faster decay), the decay rate of these reconstructed fields seems to saturate around $m \approx 1.4$, similar to theoretical predictions. This is supportive of our hypothesis that coherent modes—which we assume are removed in this reconstruction—are superimposed on top of stochastic turbulence. After removal of those coherent modes, indeed the stochastic content decays as expected.

We note the two outliers in the latter dataset (i.e. the two cases at $Ro > 1.7$) which have decay rates within the expected range but markedly lower than the other cases. These two high-Ro cases are the original low-Ro cases with the strongest applied power gradient. The strong shift in Rossby number indicates the efficient removal of (coherent) vortical content from these cases. The lower decay rate for the remaining stochastic content of these cases highlights an important caveat of the applied method: while removal of POD modes can "clean up" a velocity field, it does not recover pristine stochastic turbulence. One reason is that the coherent modes can displace, distort or modulate the stochastic content, analogous to frequency and amplitude modulation in wall-bounded turbulence (see, e.g. Mathis *et al.* 2009; Ganapathisubramani *et al.* 2012). As such, even when separated perfectly, the reconstructed stochastic content is not free from the influence of the coherent modes. In addition, the distinction between stochastic and coherent modes is somewhat ambiguous—and the difference between the two is potentially only statistical rather than physical.

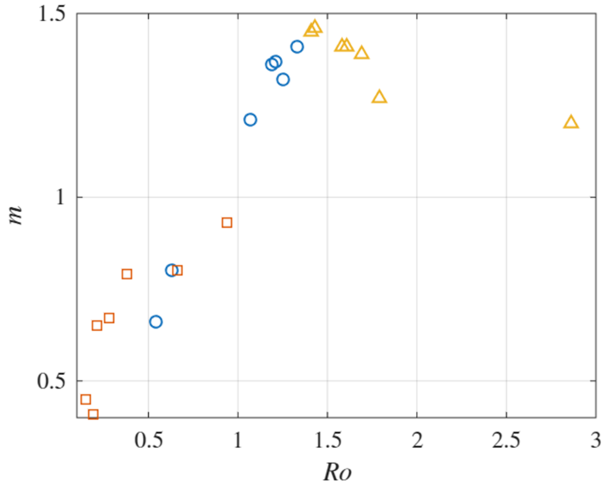

Figure 8: Fitted decay coefficient m as function of Rossby number Ro for all seven cases. Blue circles: full velocity fields; orange squares: reconstructed "coherent" velocity fields; yellow triangles: reconstructed "stochastic" velocity fields.

CONCLUSIONS

The present results demonstrate that the apparent variability in turbulent kinetic energy (TKE) decay rates can arise from the presence of coherent structures in the flow. By introducing controlled asymmetry in a synthetic-jet-driven turbulence facility, we generate flows with increasing coherent vortical content—characterized using a modified Rossby number—leading to a systematic reduction in the measured decay exponent from $m \approx 1.4$ to $m \approx 0.66$.

A POD-based decomposition framework was developed to isolate these effects. By identifying modes that are both slow-decaying and correlated across realizations, we separate coherent structures from the stochastic turbulence. Removal of these modes yields reconstructed velocity fields that retain most of the turbulent energy while exhibiting decay exponents in the range $m = 1.2$–1.45, consistent with classical expectations.

These findings suggest that reduced decay rates are not the result of a global modification of turbulence dynamics, but are instead driven by a small number of energetic coherent modes that persist over long timescales. As such, the presence of coherent structures can bias conventional estimates of TKE decay, providing a plausible explanation for the spread of decay exponents reported in the literature.

More broadly, this work suggests that careful separation of coherent and stochastic contributions is necessary when assessing turbulence decay, particularly in laboratory flows where large-scale organization may be unintentionally introduced.

RELATED PUBLICATION

Related results are published in our recent paper Gautam & Berk (2026).

REFERENCES

Bellani, Gabriele & Variano, Evan A 2014 Homogeneity and isotropy in a laboratory turbulent flow. *Experiments in fluids* **55** (1), 1646.

Butcher, Daniel & Spencer, Adrian 2019 Cross-correlation of pod spatial modes for the separation of stochastic turbulence and coherent structures. *Fluids* **4** (3), 134.

Carter, Douglas, Petersen, Alec, Amili, Omid & Coletti, Filippo 2016 Generating and controlling homogeneous air turbulence using random jet arrays. *Experiments in Fluids* **57** (12), 189.

Esteban, L Blay, Shrimpton, JS & Ganapathisubramani, Bharathram 2019 Laboratory experiments on the temporal decay of homogeneous anisotropic turbulence. *Journal of Fluid Mechanics* **862**, 99–127.

Ganapathisubramani, B., Hutchins, N., Monty, J. P., Chung, D. & Marusic, I. 2012 Amplitude and frequency modulation in wall turbulence. *Journal of Fluid Mechanics* **712**, 61–91.

Gautam, Ankit & Berk, Tim 2026 Quantifying the impact of coherent structures on the turbulent kinetic energy decay rate: A proper orthogonal decomposition approach. *Physical Review Fluids* **11** (4), 044906.

Goepfert, C., Marié, J.L., Chareyron, D. & Lance, M. 2010 Characterization of a system generating a homogeneous isotropic turbulence field by free synthetic jets. *Exp Fluids* **48**, 809–822.

Gorce, Jean-Baptiste & Falcon, Eric 2023 Statistics of a two-dimensional immersed granular gas magnetically forced in volume. *Phys. Rev. E* **107**, 034903.

Hearst, R. J. & Lavoie, P. 2014 Decay of turbulence generated by a square-fractal-element grid. *Journal of Fluid Mechanics* **741**, 567–584.

Hwang, W & Eaton, JK 2004 Creating homogeneous and isotropic turbulence without a mean flow. *Experiments in Fluids* **36** (3), 444–454.

John, John Panickacheril, Donzis, Diego A & Sreenivasan, Katepalli R 2022 Laws of turbulence decay from direct numerical simulations. *Philosophical Transactions of the Royal Society A* **380** (2218), 20210089.

Kolmogorov, Andrej Nikolaevich 1941 On degeneration (decay) of isotropic turbulence in an incompressible viscous liquid. In *Dokl. Akad. Nauk SSSR*, , vol. 31, pp. 538–540.

Lavoie, P., Djenidi, L. & Antonia, R. A. 2007 Effects of initial conditions in decaying turbulence generated by passive grids. *Journal of Fluid Mechanics* **585**, 395–420.

Mathis, Romain, Hutchins, Nicholas & Marusic, Ivan 2009 Large-scale amplitude modulation of the small-scale structures in turbulent boundary layers. *Journal of Fluid Mechanics* **628**, 311–337.

Nezami, Arefe Ghazi, Byron, Margaret & Johnson, Blair A 2023 Laboratory generation of zero-mean-flow homogeneous isotropic turbulence: Non-grid approaches. *Flow* **3**, E42.

Saffman, PG 1967 The large-scale structure of homogeneous turbulence. *Journal of Fluid Mechanics* **27** (3), 581–593.